JOURNAL OF CATALYSIS 127, 706–718 (1991)

Acid Strength of Silica-Supported Oxide Catalysts Studied by Microcalorimetric Measurements of Pyridine Adsorption

NELSON CARDONA-MARTÍNEZ[1] AND J. A. DUMESIC[2]

Department of Chemical Engineering, University of Wisconsin, Madison, Wisconsin 53706

Received March 8, 1990; revised July 9, 1990

Microcalorimetric measurements of the differential heat of pyridine adsorption were used to probe the distribution of acid strength on a series of silica-supported oxide catalysts. Depositing oxides of the following cations onto silica increased the acid strength of the catalyst: Ga^{3+}, Zn^{2+}, Al^{3+}, Fe^{3+}, Fe^{2+}, Mg^{2+}, and Sc^{3+}. The acid strength distribution curves for the supported oxide samples showed either two or three regions of constant heat of adsorption while silica had an energetically homogeneous surface. The Ga, Al, and Sc samples were found to have both Brønsted and Lewis acidity while the remaining samples showed only Lewis acidity. Incremental adsorption of pyridine indicated that the initial region of highest heat corresponds to strong Lewis acidity while intermediate heats seemed to be due to weaker Lewis acid sites or a combination of Lewis and Brønsted acid sites. The final region of lowest heat was due to H-bonded pyridine on silica. Estimates of the entropies of adsorption were determined, providing information about the mobility of the adsorbed pyridine molecules. The initial differential heat of adsorption increases proportionally to the Sanderson electronegativity of the added oxide.

INTRODUCTION

In a previous publication (*1*) we discussed the acid properties of silica and silica–alumina in terms of the differential heat of pyridine adsorption on these surfaces. Here we extend that study and present results for a series of silica-supported oxides with a wide range of electronegativities.

According to Tanabe, the acid-base properties of mixed metal oxides can be varied by choosing different metal oxide constituents at different concentrations and by changing the treatment of the sample (*2*). Thus, it appears that by properly choosing the aforementioned variables, mixed oxides could be used to develop materials with desired acid-base properties. The present work explores this concept for a series of silica-supported oxides. Several criteria led us to choose this series of materials. The character of the support oxide must be acidic or at least not strongly basic; e.g., MgO has been shown to have no acid sites and strong basicity (*3–5*), and doping this basic support with iron does not generate acidity (*3*). In contrast, depositing MgO onto SiO_2 creates new acid sites (*6, 7*). If the number of acid sites on the host oxide alone is too high, however, the effect of adding a small amount of dopant is not easy to identify. Addition of iron to alumina, the latter of which has a large number of acid sites, generates a small number of new sites not easily distinguishable from the original sites (*3*). Silica is an ideal host oxide due to its absence of strong acidity, high surface area, and acidic character, which allow for unequivocal measurement of the acidity created by adding the dopant. Its electronegativity is high and the oxygen coordination is two, which leads to the existence of coordinatively unsaturated dopant cations on the surface (*8*).

One of the objectives of this study was to

[1] Present address: University of Puerto Rico, College of Engineering, Chemical Engineering Department, P.O. Box 5000, Mayagüez, P.R. 00709-5000.

[2] To whom correspondence should be addressed.

0021-9517/91 $3.00

investigate the effect on acid properties of the electronegativity of the added dopant. For two cations in similar coordination and bonding sites, one would expect the cation with higher electronegativity to be a stronger Lewis acid site (*8*). To make this type of comparison we need to maintain constant as many of the other properties of the systems as possible. Hence, the host lattice (SiO_2) and the loading, in atoms of dopant per m^2 of catalyst, were held constant and the dopant cation varied. Small quantities of the dopants on silica were used so as not to alter the bulk properties of the catalysts, e.g., the overall structure and surface area. Two criteria were used to choose the dopant cations: their size should be similar to that of silicon, and they should have considerably different electronegativities. Accordingly, oxides of the following cations were deposited onto silica: Mg, Sc, Fe, Al, Zn, and Ga. Table 1 presents a summary of the properties of these dopant cations and oxides.

TABLE 1

Summary of Properties of the Cations Deposited onto SiO_2[a]

Cation	Loading	S_{oxide}[b]
Mg^{2+}	1.43	2.19
Sc^{3+}	1.89	2.30
Fe^{2+}	1.41	2.47
Fe^{3+}	1.41	2.67
Al^{3+}	1.46	2.70
Zn^{2+}	1.44	2.85
Ga^{3+}	1.28	3.10
SiO_2	78.5[c]	3.06

[a] Loading in units of cations/$m^2 \times 10^{17}$.

[b] S_{oxide} ≡ Sanderson electronegativity of the oxide (*39*, *40*).

[c] Surface silicon atoms from Ref. (*9*).

EXPERIMENTAL

Sample Preparation and Pretreatment

Samples were prepared by incipient wetness impregnation utilizing 1 ml of solution per gram of SiO_2. The silica (Cab-O-Sil grade S-17) was X-ray amorphous (*9*) with a measured BET surface area of 400 $m^2 g^{-1}$. It contained less than 38 ppm total metallic impurities (*9*) and was used without further purification. The small quantities of dopant oxides used did not change the surface area of the catalysts. All samples were prepared using nitrate salts in aqueous solution followed by drying in air at 390 K for 24 h and calcination in air for 4 h at 723 K. The magnesium, iron, aluminum, zinc, and gallium nitrates used were high-purity materials (99.999%) from Aldrich Chemicals (Milwaukee, WI) and scandium nitrate was 99.9% pure from Alfa Products (Massachusetts).

The loading was kept nearly constant at 1.4×10^{17} atoms of dopant per m^2 of catalyst surface area. This loading corresponds to 1.8% of the silicon atoms on the surface. The samples were chemically analyzed by Galbraith Laboratories to determine the actual loadings, which are summarized in Table 1.

All the samples (except for Fe) were pretreated by oxidation in flowing oxygen at 723 K for 4 h followed by evacuation for 2 h at the treatment temperature. The iron samples were pretreated by reduction in flowing hydrogen at 673 K for 4 h followed by evacuation. This treatment yields Fe^{2+}. The treatment temperature of iron was lower because of the formation of metallic iron particles observed with Mössbauer spectroscopy at higher temperatures (*8*). To obtain Fe^{3+}, the sample was subsequently oxidized in flowing oxygen at 473 K for 4 h. These pretreatments ensure that the desired oxidation state of the dopant is present on the surface.

Microcalorimetric Measurements of Heats of Adsorption

The adsorption and desorption of pyridine was monitored calorimetrically to ascertain the number and strength of acid sites present. The heats of adsorption and related values were measured in a microcalorimetry apparatus that allows conventional adsorp-

tion isotherm and calorimetric data to be collected simultaneously. A detailed description of the apparatus and procedure has been given previously (*1, 10*).

Pyridine Adsorption on Silica and Silica/Alumina

Microcalorimetric results for pyridine adsorption on silica at 473 K have been discussed in a previous publication (*1*). Briefly, it was found that the silica surface is energetically homogeneous for the extents of coverage studied giving an approximately constant differential heat of adsorption of 95 kJ mol^{-1}. This heat is considerably higher than the heat of condensation of pyridine, 35.1 kJ mol^{-1} (*11*) and compares favorably with the initial differential heat of adsorption of 94 kJ mol^{-1} reported by Kiselev and coworkers (*12*) for the adsorption of pyridine on a macroporous silica–aerosilogel after evacuation at 473 K. Using statistical mechanics and the volumetric adsorption data we estimated an activation energy for surface diffusion of approximately 20 kJ mol^{-1}, which indicated that under these conditions pyridine retains a significant fraction of its mobility. This result is consistent with ^{13}C NMR spectroscopy which indicated that pyridine adsorbed on silica is in a state of rapid motion even at 301 K (*13*). The results for pyridine adsorption on silica are included in Figs. 1 through 4 as reference values for comparison with the results of the silica-supported oxides.

The results for pyridine adsorption on silica-supported aluminum oxide at 473 K were also discussed previously (*1*). In short, depositing alumina on SiO_2 increased the acidity of the catalyst considerably. The integral and differential heats of adsorption for pyridine adsorbed on silica-supported aluminum oxide at 473 K are included in Figs. 3 and 4. The initial differential heat of pyridine adsorption was determined to be 219 kJ mol^{-1}. Adsorption at 473 K yields three regions of nearly constant heats of adsorption with an intermediate sharp step near 170 kJ mol^{-1}. The experimental integral heat data were fit using the Langmuir model for three sites as described in Ref (1). This model describes the dependence of the differential heat of adsorption on the amount adsorbed on a surface with discrete sites and is equivalent to the model discussed by Klyachko (*14*). The only difference in our development is that we do not constrain the entropy of adsorption to be identical on all sites. This allows for differences in mobilities among molecules adsorbed on different types of sites. Using statistical mechanics and the calculated entropies of adsorption we can then estimate qualitatively the fractional losses of translational and rotational degrees of freedom of the molecules adsorbed on a given type of site (*1*). As seen later we have evidence that indicates that adsorption on the strongest sites of some of our samples is irreversible. The calculated entropies for adsorption on these sites are then questionable because the thermodynamic model is not applicable under these conditions and are presented only for qualitative comparison.

For the proposed model, if there are s sites on the surface, the coverage will be given by

$$\theta = \sum_{i=1}^{s} \theta_i = \sum_{i=1}^{s} \frac{\chi_i K_i p}{1 + K_i p} = \sum_{i=1}^{s} \frac{n_i}{n_m}, \quad (1)$$

where χ_i is the fraction of centers i and n_i and n_m are the amount adsorbed on site i (i.e., μmol g^{-1} or μmol m^{-2}) and the maximum adsorption capacity, respectively. In terms of the differential heat of adsorption on site i, q_i, the integral heat of adsorption, Q, is given by

$$Q = \sum_{i=1}^{s} q_i n_i = \sum_{i=1}^{s} \frac{n_1 n_{im} q_i}{n_1 m \alpha_{1,i} - n_1(\alpha_{1,i} - 1)}, \quad (2)$$

where $\alpha_{1,i}$, is a selectivity or distribution coefficient and is defined as

TABLE 2

Summary of Parameters for Fit of Integral Heat of Pyridine Adsorption on Silica-Supported Metal Oxides[a]

Cation	S_{oxide}	n_{1m} (μmol g^{-1})	q_1 (kJ mol^{-1})	ΔS_1 (J/mol-K)	n_{2m} (μmol g^{-1})	q_2 (kJ mol^{-1})	ΔS_2 (J/mol-K)
Mg^{2+}	2.19	6.0	146.3 ± 1.0	−180 ± 3	6.0	111.8 ± 1.6	−155 ± 3
Sc^{3+}	2.30	4.5	164.5 ± 2.4	−219 ± 13	18.5	133.8 ± 1.0	−193 ± 13
Fe^{2+}	2.47	9.2	182.0 ± 0.5	−267 ± 3	9.0	134.4 ± 0.8	−198 ± 3
Fe^{3+}	2.67	13.4	208.4 ± 0.5	−321 ± 3	13.8	188.1[b]	−319 ± 3
Al^{3+}	2.70	12.7	219.9 ± 0.5	−330 ± 6	14.8	177.1 ± 0.7	−289 ± 6
Zn^{2+}	2.85	12.9	235.2 ± 0.3	−358 ± 8	25.3	162.0 ± 0.3	−245 ± 8
Ga^{3+}	3.10	8.2	290.0 ± 0.5	−437 ± 10	19.3(4.5)[c]	138(121)[c]	−161(−188)[c]

[a] Typical values for site 3 are: n_{1m} = 140 μmol g^{-1}, q_3 = 95 kJ mol^{-1}, and ΔS_3 = − 167 J mol^{-1} K^{-1}. The gas phase absolute entropy of pyridine at 473 K is 328 J mol^{-1} K^{-1} (*11*). Confidence intervals, 95%, are shown for q_i and ΔS_i.

[b] Value questionable because differential heat curve decreased continuously with no intermediate step or inflection point.

[c] Values for fourth site in parenthesis.

$$\alpha_{1,i} = \frac{K_1}{K_i} = \exp\left\{\frac{\Delta S_1 - \Delta S_i}{R}\right\} \exp\left\{\frac{q_1 - q_i}{RT}\right\}. \quad (3)$$

For large differences among the equilibrium constants the different types of sites are filled successively.

To obtain the fit for adsorption on Al_2O_3/SiO_2, as well as other fits in this work, the values found for silica were assigned to the third site or allowed to vary near those values. A summary of the results for adsorption on Al_2O_3/SiO_2 at 473 K, as well as the results for the other samples studied in this work, is presented in Table 2.

Pyridine Adsorption on Magnesium Supported on Silica

Magnesia has strong and numerous basic sites but no acid sites (e.g., *5, 15–17*). However, when magnesia is added to silica, acidity is generated (*7*). This acidity is exclusively of the Lewis type (*6*).

Magnesium oxide was the least electronegative oxide studied with a Sanderson electronegativity, S_{MgO}, equal to 2.19. The MgO on SiO_2 sample used was analyzed to have a content of 0.23 wt% Mg, which corresponds to a loading of 1.43×10^{17} cations m^{-2}. Doping silica with magnesia produces new acid sites as illustrated by Figs. 1 and 2. These figures show the integral and differential heats of adsorption of pyridine on MgO/SiO_2 samples at 473 K. The results for only one run are presented for simplicity, but the experiment was duplicated with good reproducibility (better than ±1 kJ mol^{-1}). The complete data set was used to obtain the fit. The same procedure is used for the other systems studied in this work

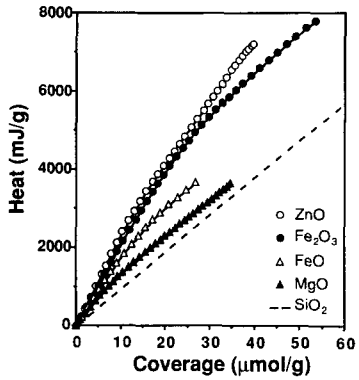

FIG. 1. Integral heat of adsorption for pyridine adsorbed on silica-supported oxides that showed only Lewis acidity.

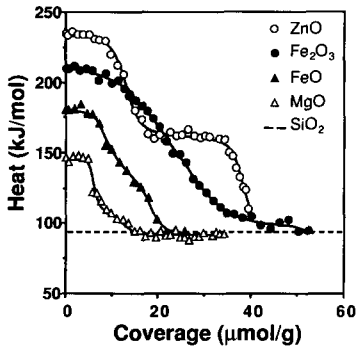

FIG. 2. Differential heat of adsorption for pyridine adsorbed on silica-supported oxides that showed only Lewis acidity.

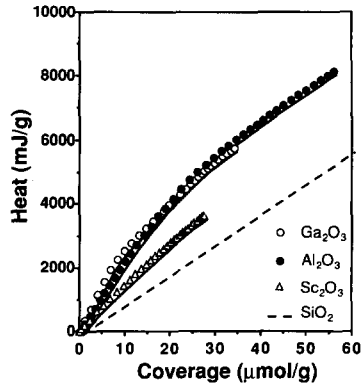

FIG. 3. Integral heat of adsorption for pyridine adsorbed on silica-supported oxides that showed both Lewis and Brønsted acidity.

using results from at least two experiments per system. The initial differential heat of pyridine adsorption on MgO/SiO_2 at 473 K is calculated from the integral heat curve as 146 kJ mol^{-1}. The plot of differential heat of pyridine adsorption on silica-magnesia does not show an intermediate step as on Al_2O_3/SiO_2; instead, the differential heat decreases continuously indicating that the surface is more heterogeneous. The calorimetric data cannot be fitted adequately with only two sites. Hence, using the same procedure as for silica–alumina, the integral heat results were fitted using three sites. The parameters found are summarized in Table 2.

The fit found is good statistically, but there is one physical inconsistency: the entropy change of adsorption for site 2 is slightly smaller than the entropy for site 3. This might be because more than one site is needed to describe the intermediate coverage on the MgO/SiO_2 surface. The estimated entropy of adsorption for site 1 indicates a 55% loss of the pyridine gas phase entropy at 473 K and, using the same procedure and molecular dimensions used for silica (*1*), this corresponds to approximately an 80% loss of translational freedom and a 50% loss of rotational freedom. Hence, pyridine adsorbed on the strongest sites on MgO/SiO_2 retains some mobility.

Pyridine Adsorption on Scandium Supported on Silica

Scandium has been shown to enhance the acidity of silica and to generate both Lewis and Brønsted sites (*6*). The electronegativity of scandium oxide is 5% higher than that of MgO, $S_{Sc_2O_3} = 2.30$. The loading of the sample used was 0.56 wt% Sc, which corresponds to 1.89×10^{17} cations m^{-2}. The generation of new acid sites on silica is shown by the calorimetric results in Figs. 3 and 4. The integral and differential heats of adsorption of pyridine on Sc_2O_3/SiO_2 at 473 K are shown in these figures. The initial differential heat of pyridine adsorption on $Sc_2O_3/$

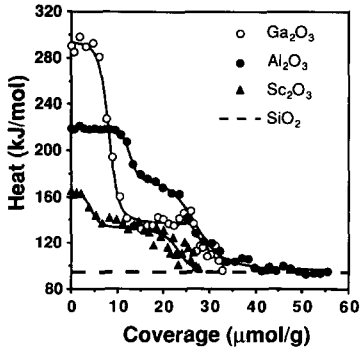

FIG. 4. Differential heat of adsorption for pyridine adsorbed on silica-supported oxides that showed both Lewis and Brønsted acidity.

SiO_2 at 473 K is calculated from the integral heat curve as 163 kJ mol^{-1}. The plot of differential heat of pyridine adsorption on scandia supported on silica displays an intermediate step at about 135 kJ mol^{-1}. As for other samples studied in this work, the differential heat of adsorption dropped to the value found for the adsorption on silica. There was no evidence that the differential heat dropped below the value found for silica for the extents of coverage studied. The parameters found after fitting the integral heat data with the Langmuir model are given in Table 2. All the parameters are physically reasonable. Pyridine adsorbed on site 1 has lost over 90% of its translational freedom, almost 80% of its rotational freedom, and hence most of its mobility. The entropy of adsorption for site 2 corresponds to a 58% loss of the pyridine gas phase entropy giving about an 85% loss of translational freedom and a 60% loss of rotational freedom. Hence, pyridine adsorbed on the site 2 of Sc/SiO_2 retains some of its mobility.

Pyridine Adsorption on Iron Supported on Silica

It has been shown with Mössbauer spectroscopy that addition of iron oxide to silica produces iron cations in low coordination environments and that these new sites are acidic (*8*). The acidity was found to be exclusively of the Lewis type (*6, 8*). Ferrous and ferric cations on silica were also found to have different acidities and acid strengths.

Both forms of iron oxide studied here have intermediate electronegativities between those values of scandia and alumina, Fe_2O_3 being more electronegative ($S_{Fe_2O_3}$ = 2.67) than FeO (S_{FeO} = 2.47). The samples contained 0.52 wt% Fe, which corresponds to 1.41×10^{17} cations m^{-2}. The generation of new acid sites on silica is shown by the calorimetric results in Figs. 1 and 2. These figures show the integral and differential heats of adsorption of pyridine at 473 K on Fe^{2+}/SiO_2 and Fe^{3+}/SiO_2.

The initial differential heat of pyridine adsorption at 473 K, calculated from the initial slopes of the integral heat plots, are 210 and 180 kJ mol^{-1}, respectively, on Fe^{3+}/SiO_2 and Fe^{2+}/SiO_2. The reduced form of iron oxide has considerably fewer and weaker acid sites than the oxidized form of iron. Both the integral and differential heat curves for Fe^{2+}/SiO_2 fall below those for Fe^{3+}/SiO_2 over the range of coverage studied. Neither sample displays a definite step in the plots of differential heat of adsorption at intermediate coverages, and the curves decrease continuously indicating the presence of heterogeneous acid strength distributions. The acid strength distribution curve for divalent iron shows a high concentration of sites at 135 kJ mol^{-1} and no sites higher than 181 kJ mol^{-1}, while trivalent iron shows a large concentration of sites near 208 kJ mol^{-1} and low concentration of sites with intermediate strength. The parameters found after fitting the integral heat data with the Langmuir model are given in Table 2. The calculated entropies of adsorption for sites 1 and 2 on Fe^{3+}/SiO_2 represent a loss of approximately 97% of the gas phase entropy indicating irreversible adsorption on these sites. This was confirmed by a second adsorption on Fe^{3+}/SiO_2 after evacuation overnight at 473 K. Specifically, no sites with differential heats higher than 120 kJ mol^{-1} were observed under these conditions indicating that most of the pyridine is adsorbed irreversibly. For Fe^{2+}/SiO_2, pyridine adsorbed on site 1 loses about 80% of its gas phase entropy. Adsorption on the second site yields a 60% loss of the gas phase entropy which represents approximately a 90% loss of translational freedom and a 60% loss of rotational freedom.

Pyridine Adsorption on Zinc Supported on Silica

In spite of its high electronegativity (S_{ZnO} = 2.85), zinc oxide is considered a solid base for most applications (*16, 18–20*). Nevertheless, its acidic properties have also been established (*21*). When zinc oxide is added to silica, new acid sites are generated, and they are of the Lewis type (*6*).

The sample used in this study had 0.62 wt% Zn, which corresponds to a loading of 1.44×10^{17} cations m^{-2}. The enhancement in acidity upon addition of ZnO to silica is demonstrated in Figs. 1 and 2. These figures show the integral and differential heats of adsorption of pyridine on ZnO/SiO_2 samples at 473 K. The initial differential heat of pyridine adsorption on ZnO/SiO_2 at 473 K is calculated from the integral heat curve as 235 kJ mol^{-1}. The plot of differential heat of pyridine adsorption on ZnO/SiO_2 shows significant steps near 235 and 160 kJ mol^{-1} indicating the presence of several energetically homogeneous sites. The parameters found after fitting the integral heat results with the Langmuir model are presented in Table 2. In this case, a value of ΔS for site 3 equal to about -180 J mol^{-1} K^{-1} is needed to fit the isotherm, this value being different from the value of -167 J mol^{-1} K^{-1} characteristic of silica. Another problem seen with the fit is that the entropy of adsorption for site 1 is higher than the gas phase pyridine entropy. These results can be rationalized by noting the large value for the initial differential heat of adsorption which is higher than the maximum value calculated to attain the thermodynamic distribution of surface sites in Ref. (*1*) (215–235 kJ mol^{-1}). Therefore, an equilibrium model is not applicable, and the differential heats at low coverages could be an average from different sites. In any case, such a large entropy of adsorption indicates a strong interaction with the surface and immobile adsorption. The calculated entropy of adsorption for site 2 also corresponds to immobile adsorption.

Pyridine Adsorption on Gallium Supported on Silica

Gallium oxide was the most electronegative oxide studied in this work ($S_{Ga_2O_3} = 3.10$) even more electronegative than silica ($S_{SiO_2} = 3.06$). It has been demonstrated that when gallia is added to silica, strong acid sites are generated and that both Lewis and Brønsted sites are present on the surface (*4, 6*).

The sample studied contained 0.59 wt% Ga, which corresponds to a loading of 1.28×10^{17} cations m^{-2}. The enhancement in acidity upon addition of Ga_2O_3 to silica is shown in Figs. 3 and 4. The integral and differential heats of adsorption of pyridine on Ga_2O_3/SiO_2 samples at 473 K are shown in these figures. The initial differential heat of pyridine adsorption on Ga_2O_3/SiO_2 at 473 K is calculated from the integral heat curve as 286 kJ mol^{-1}. The plot of differential heat of pyridine adsorption on Ga_2O_3/SiO_2 shows steps near 286 and 138 kJ mol^{-1} indicating the presence of several energetically homogeneous sites. The integral heat results cannot be adequately fitted with three sites; however, an adequate statistical fit is obtained by using four sites. The parameters found are summarized in Table 2.

As for the ZnO/SiO_2 sample, a value of ΔS for site 4 near -180 J mol^{-1} K^{-1} is needed to bring the fitted and experimental isotherms together. For Ga_2O_3/SiO_2, the entropy of adsorption for site 1 is even higher than that for ZnO/SiO_2. These results can thus also be explained by the large value for the initial differential heat of adsorption which is higher than the maximum value estimated to attain the thermodynamic distribution of surface sites. Therefore, an equilibrium model is not applicable, and the data at low coverages may represent several sites. The calculated entropies of adsorption for sites 2 and 3 correspond to losses of 80 and 85% of the translational freedom and 40 and 60% of the rotational freedom, respectively.

DISCUSSION

The results of this study show that depositing various oxides onto silica increases the acid strength of the catalyst. The heat of adsorption at low extents of adsorption is dominated by the interaction of the probe molecule with the strongest acid sites on the surface (i.e., leading to the highest differential heat of adsorption) while the contributions from weaker sites become more important as the extent of adsorption increases. When the adsorbed molecules have sufficient energy to attain thermodynamic equilibrium, then the shape of a plot

of differential heat of adsorption versus extent of pyridine adsorption provides a measure of the distribution of acid site strength on the surface (*1, 10*). Measurements of this type are of fundamental importance in understanding the catalytic properties of metal oxides. For example, acid or base sites which are too weak may not activate reactants while acid or base sites which are too strong may be irreversibly poisoned by adsorbed species. Therefore, it is important that true acid strength distributions are determined if calorimetric results are to be used to interpret and/or predict catalytic behavior.

As discussed in Ref. (*1*), surface diffusion plays an important role for the equilibration of pyridine on silica-supported oxides. Specifically, the presence of a support like silica, where adsorbed pyridine retains a significant fraction of its mobility at 473 K, helps in the equilibration of pyridine between strong sites. We estimated the activation energy for surface diffusion of pyridine on silica at 473 K to be 20 kJ mol^{-1}, and we estimated that the strongest acid site on silica that could be studied at 473 K in an equilibrium manner was 215–235 kJ mol^{-1}. This value corresponds to the initial differential heat of pyridine adsorption observed on ZnO/SiO_2.

All the samples studied in this work were adequately described with a Langmuir model employing three sites, except for the Ga_2O_3 sample which needed four sites for the Fe^{3+} sample which did not show a definite inflection point at intermediate coverages and would have required a larger number of sites to be fitted adequately. Differential heats of adsorption, acid strength distribution plots, and entropies of adsorption were determined from these fits. The results for differential heat and site energy distribution plots were shown to be model-independent by comparing them to the results found with a polynomial model. The calculated entropies of adsorption with the Langmuir model were within physically realistic values, except for the ZnO and Ga_2O_3 specimens. The entropies for site 1 on these samples were higher than the pyridine gas phase entropy at 473 K, which suggests a strong irreversible adsorption. A close look at Table 2 also shows that our results follow the generally observed compensation effect (*22, 23*) in which the entropy of adsorption increases linearly with an increase in the differential heat of adsorption.

A summary of the calorimetric results as a function of the Sanderson electronegativity of the oxide is presented in Table 3. The summary includes the initial differential heats calculated from initial slopes of integral heat plot, the differential heats for sites 1 and 2 calculated with the Langmuir model and the values of integral heat of adsorption when the differential heat drops to 96 kJ mol^{-1}. The initial differential heat of adsorption increases proportionally to the Sanderson electronegativity of the added oxide as shown in Fig. 5. Since the initial differential heat of adsorption characterizes the strongest interaction between the probe molecule and the surface, it is a good measure of the acid strength of the catalyst. There is extensive evidence in the literature that Lewis acidity is generally stronger than Brønsted acidity (*24–28*), and this was shown in particular for our samples in Refs. (*1*) and (*6*). Specifically, infrared spectroscopy results for incremental pyridine adsorption on silica–alumina showed only pyridine adsorbed on Lewis acid sites for the low coverages. Hence, the initial differential heat of adsorption corresponds to adsorption on Lewis acid sites. The correlation observed in Fig. 5 has physical significance because both electronegativity and Lewis acid strength are defined as the electron accepting strength, and they should correlate.

The interpretation of the heats of adsorption for site 2 is not as clear as for site 1. For samples that showed only Lewis acidity, site 2 corresponds to weaker Lewis sites; however, for the samples that contain also Brønsted sites, it is probable that site 2 is a combination of Brønsted sites and weak Lewis sites. The IR spectroscopy results of

TABLE 3

Summary of Calorimetric Results for Pyridine Adsorption on Silica-Supported Metal Oxides

Cation	S_{oxide}[a]	$q_{initial}$ (kJ mol^{-1})[b]	q_1 (kJ mol^{-1})[c]	q_2 (kJ mol^{-1})[d]	Q_{96} (mJ g^{-1})[e]
Mg^{2+}	2.19	146.2	146.3	111.8	1779
Sc^{3+}	2.30	163.2	164.5	133.8	4269
Fe^{2+}	2.47	180.2	182.0	134.4	3562
Fe^{3+}	2.67	209.8	208.4	188.1[f]	7639
Al^{3+}	2.70	219.0	219.9	177.1	7386
Zn^{2+}	2.85	234.9	235.2	162.0	8100
Ga^{3+}	3.10	286.2	290.0	138.1	6380
SiO_2	3.06	95.3	96.7		

[a] Sanderson electronegativity of the oxide.
[b] Initial differential heat calculated from initial slope of integral heat plot.
[c] Differential heat for site 1 calculated with Langmuir model.
[d] Differential heat for site 2 calculated with Langmuir model.
[e] Value of integral heat of adsorption when differential heat drops to 96 kJ mol^{-1}.
[f] Value questionable because differential heat curve decreased continuously with no intermediate step or inflection point.

pyridine adsorbed on silica–alumina do not provide conclusive evidence to decide whether the Brønsted and weak Lewis sites have sufficiently different heat to be resolved calorimetrically (*1*). Klyachko *et al.* (*29*) studied the acidic properties and catalytic cracking activity of a series mordenite and pentasil-type zeolites using IR spectroscopy and adsorption microcalorimetry of NH_3. They found both strong and weak Lewis acid sites as well as Brønsted sites with intermediate strength between those of the two types of Lewis acid sites. These researchers also found that the catalytic activity correlated with the acidity of the intermediate acid strength sites but no correlation was found between catalytic activity and the total acidity of the catalysts. Greppi and Dumesic (*30*) studied the activity of isopropanol dehydration on the same samples studied in this work. They found that the samples that showed only Lewis acid sites were inactive for this reaction or were from one to two orders of magnitude less active than the samples that showed Brønsted acidity. The activity of the latter samples increased in the order Sc < Ga < Al. This is the same order found for q_2 and, as illustrated in Fig. 6, a good correlation between the heats and the activity if found. No correlation was found with the initial heats or for the samples that showed only Lewis acidity. These results suggest that either the Brønsted sites have the same heat of adsorption as the weak Lewis sites on the silica-supported Sc_2O_3, Ga_2O_3, and Al_2O_3 samples or

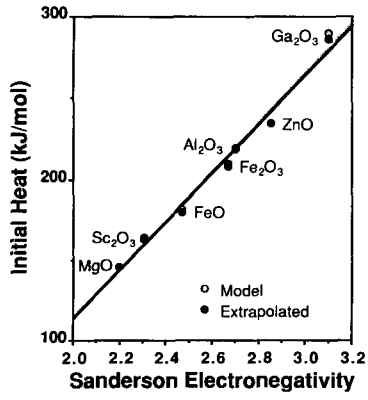

FIG. 5. Initial differential heat of pyridine adsorption as a function of the Sanderson electronegativity of the doped cation (○, differential heat for site 1 as calculated with the Langmuir model; ●, differential heat calculated from the initial slope of the integral heat versus coverage plot).

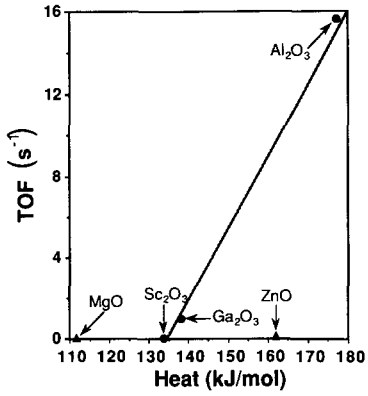

FIG. 6. Activity for isopropanol dehydration at 523 K from Ref. (*30*) as a function of the differential heat of pyridine adsorption for site 2 calculated with the Langmuir model. The turnover frequency is expressed in units of molecules/(sites corresponding to monolayer coverage for site 2)/s. Circles: samples that showed Brønsted acidity; triangles: samples that showed only Lewis acidity.

that site 2 in the differential heat of adsorption corresponds to Brønsted sites exclusively.

The integral heat of adsorption is a measure of the total acidity of the sample. In Fig. 7, we present a plot of the average integral heat of pyridine adsorption at the coverage when the differential heat of adsorption decreases to 96 kJ mol^{-1}, as a function of the Sanderson electronegativity of the doped cation. The average integral heat was determined by dividing the integral heat at q = 96 kJ mol^{-1} (Q_{96} in Table 3) by the coverage at the same differential heat (n_{96} in Table 4). In general, the average integral heat increases with electronegativity, except for the case of Ga_2O_3/SiO_2. The low value for this latter sample is due to the large number of weaker sites (probably Brønsted acid sites) that exist in addition to the very strong Lewis acid sites. It is clear that correlations involving the differential heat of adsorption (e.g., Fig. 5) should be superior to those involving the average integral heat, since the variation in differential heat with coverage provides information about the acid site distribution.

Volumetric and thermokinetic results for pyridine adsorption on silica-supported metal oxides are summarized in Table 4. This summary presents the coverages obtained when the differential heat decreases to 96 kJ mol^{-1}, concentrations of sites 1 and 2 calculated with the Langmuir model, the coverages for the maximum in the thermokinetic parameter plot, and, for comparison, the coverages after evacuation at 473 K for 1 h, interpolated from data at 423 and 523 K from Ref. (*4*). In this context it should be noted that the thermokinetic parameter is defined in terms of the time over which the heat is evolved after each successive dose of pyridine onto the sample. Generally, the thermokinetic parameter first increases with pyridine coverage on the sample, passes through a maximum, and then decreases with further increase in coverage.

The coverage at which the differential heat decreases to 96 kJ mol^{-1} provides an estimate of the amount of pyridine adsorbed on the supported oxide, and with this we can estimate the fraction of the added cations that generate acid sites. This fraction varies from about 15% of the added cations for Mg, to around 27% for Fe^{2+} and Sc, and about 50% for the other cations. A comparison of the amount of pyridine adsorbed with heats higher than 96 kJ mol^{-1} with the reported amounts of irreversibly adsorbed pyridine determined gravimetrically after evacuation at 473 K indicates that for most samples the calorimetric results are lower than the gravimetric results. A possible explanation of the difference is that at the conditions used for the gravimetric experiments, the time of evacuation or the pumping speed were not sufficient to desorb completely pyridine from these sites on silica. The fact that adsorbed pyridine was detected on silica even after desorption at temperatures as high as 523 K supports this explanation.

Additional insight into the adsorption process can be obtained from the shape of the individual thermograms. The time for the heat evolution for all the doses over silica

TABLE 4

Summary of Volumetric and Thermokinetic Results for Pyridine Adsorption on Silica-Supported Metal Oxides

Cation	Loading[a]	n_{96}[b]	% of L[c]	n_{1m}[d]	n_{2m}[e]	n_{TP}[f]	n_{evac}[g]
Mg^{2+}	94.8	14.6	15.4	6.0	6.0	9	19.9
Sc^{3+}	125.3	34.2	27.3	4.5	18.5	4	31.1
Fe^{2+}	93.6	26.0	27.8	9.2	9.0	10	40.5
Fe^{3+}	93.6	51.4	54.9	13.4	13.8	29	48.5
Al^{3+}	96.6	48.3	50.0	12.7	14.8	19	48.3
Zn^{2+}	95.4	48.6	50.9	12.9	25.3	8	68.4
Ga^{3+}	85.1	40.5	47.6	8.2	19.3 + 4.5[h]	4	56.1
Si–OH	250[i]	—	—	—	—	1	3.7

[a] In units of μmol of cations/g of catalyst, all the coverages are in units of μmol of pyridine adsorbed/g of catalyst.

[b] Coverage when the differential heat drops to 96 kJ mol^{-1}.

[c] Percentage of loaded cations that become acid sites.

[d] Maximum coverage for site 1 calculated with Langmuir model.

[e] Maximum coverage for site 2 calculated with Langmuir model.

[f] Coverage for maximum in the thermokinetic parameter plot.

[g] Coverage after evacuation at 473 K for 1 h, interpolated from data at 423 and 523 K from Ref. (*4*) and corrected for any difference in loading.

[h] Values corresponding to sites 2 and 3.

[i] From the pyridine saturation coverage at 423 K and 650 Pa determined gravimetrically (*31*).

was (i) short compared to that for both the initial and intermediate heat regions for the silica-supported samples and (ii) comparable to that observed for the final region of low differential heats for the supported samples. The adsorption process in this latter region and over SiO_2 appears to be reversible. This agrees with the results seen by various authors (*7, 32*) and is consistent with the discussion above dealing with surface kinetics.

From the results in Table 4 it can be seen

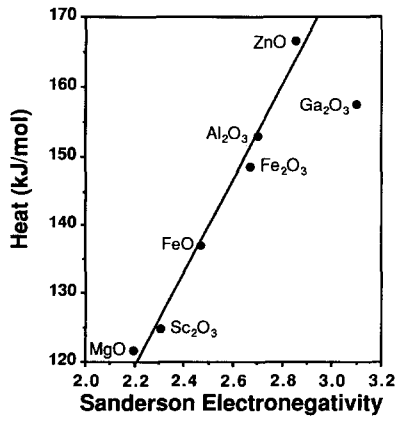

FIG. 7. Integral heat of pyridine adsorption when the differential heat of adsorption decreases to 96 kJ mol^{-1} $\{q_{av} = Q_{96}/n_{96}\}$ as a function of the Sanderson electronegativity of the doped cation.

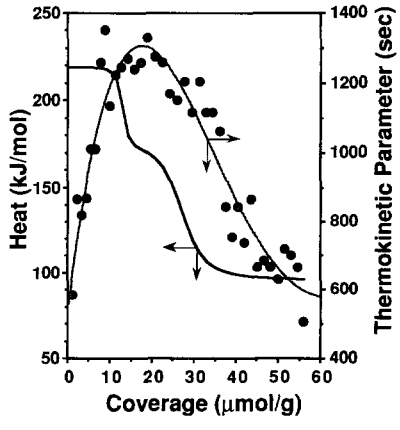

FIG. 8. Fitted differential heat of adsorption and thermokinetic parameter for pyridine adsorbed on Al/SiO_2 at 473 K after oxidation at 723 K (——, fitted heat; ●, thermokinetic parameter).

that for most samples the maximum in the thermokinetic parameter was located upon completion of filling site 1 or in the middle of filling site 2. Figure 8 shows a plot of the thermokinetic parameter and a plot of the differential heat of adsorption versus coverage for Al_2O_3/SiO_2 as an example of this behavior. The maximum is indicative of a change from strong to weaker adsorption (*33*) and its location is qualitatively consistent with the previous discussion of surface energetics. At low coverages, pyridine adsorbs on the strong sites where it is essentially irreversibly held giving a low thermokinetic parameter. For increasing coverages, a smaller fraction of the strongest sites are available and there will be a competition for the pyridine molecules between the strong and weaker sites. Furthermore, pyridine adsorbed on the weaker sites will be exchanged with other sites of similar strength or will migrate to the stronger sites. Such processes leading to surface equilibration increase the thermokinetic parameter. When most of the stronger sites are covered, the exchange of pyridine takes place among weaker sites, which is a faster process due to lower adsorption energies. The thermokinetic parameter thus decreases approaching the value characteristic of silica. The unusually large value seen for Fe^{3+} is possibly due to the wide range of sites with different energetics that appear to exist on this sample. The above discussion is consistent with the results and discussion by Kapustin and co-workers (*34*) who studied microcalorimetrically the adsorption of ammonia on Na–mordenite at 30–400°C. According to these authors the long time to establish equilibrium at intermediate coverage is caused by a slow redistribution of the NH_3 molecules on the sites that are more energetically favorable when adsorption is performed in a stepwise manner with small doses. If a sufficient amount of ammonia to adsorb on all the active sites was admitted equilibrium was reached rapidly providing supporting evidence for the above hypothesis. Increasing the adsorption temperature decreased the time to achieve thermal equilibrium indicating that the rate of NH_3 redistribution on the surface was increasing which is consistent with our interpretation of surface diffusion aided equilibration. The thermokinetic techniques have also been used to differentiate between adsorption mechanisms, between strong and weak acidity, or between reversible and irreversible adsorption by various authors (*33–38*).

CONCLUSIONS

In summary, the following conclusions can be reached from the present study:

- Surface diffusion plays an important role for equilibration of adsorbed pyridine on silica-supported samples.
- Under appropriate conditions, microcalorimetry of adsorbed pyridine provides a good measure of the acid strength distribution of the catalyst.
- Depositing metal oxides on silica increases the acidity and acid strength of the catalyst.
- The acid strength distribution of the silica-supported oxides appears to be described by adsorption on a small number of energetically homogeneous sites.
- The strength of the Lewis acidity created by depositing oxides onto silica can be correlated by the Sanderson electronegativity of the added oxide.
- It appears that the strength of the Brønsted acid sites formed by depositing Sc_2O_3, Ga_2O_3, and Al_2O_3 on silica may be related to the catalytic activity for isopropanol dehydration.

ACKNOWLEDGMENTS

We acknowledge the support of a National Science Foundation Equipment Grant that allowed us to purchase the microcalorimeter used in this work. Furthermore, we thank the Department of Energy for the partial financial support of this work (DE-FG02-84ER13183). Finally, we thank the Graduate Professional Opportunity Program and the Chevron Corporation for financial support for one of us (N.C.M.) during different stages of this work and the University of Puerto Rico–Mayagüez Campus for providing a Leave of Absence to the same author.

REFERENCES

1. Cardona-Martínez, N., and Dumesic, J. A., *J. Catal.*, in press.
2. Tanabe, K., *in* "Catalysis Science and Technology" (J. R. Anderson and M. Boudart, Eds.), Vol. 2, p. 231. Springer-Verlag, New York, 1981.
3. Connell, G., and Dumesic, J. A., *J. Catal.* **102,** 216 (1986).
4. Connell, G., Ph.D. thesis, University of Wisconsin–Madison, 1985.
5. Auroux, A., and Védrine, J. C., *in* "Catalysis by Acids and Bases," Vol. 311, Elsevier, Amsterdam, 1985.
6. Connell, G., and Dumesic, J. A., *J. Catal.* **105,** 285 (1987).
7. Masuda, T., Taniguchi, H., Tsutsumi, K., and Takahashi, H., *Bull. Chem. Soc. Japan* **51,** 1965 (1978).
8. Connell, G., and Dumesic, J. A., *J. Catal.* **101,** 103 (1986).
9. Cabot Corporation, "Cab-O-Sil Properties and Functions," 1985.
10. Cardona-Martínez, N., Ph.D. thesis, University of Wisconsin–Madison, 1989.
11. Dean, J. A., "Langes's Handbook of Chemistry," 12th ed., McGraw–Hill, New York, 1979.
12. Curthoys, G., Davydov, V. Ya., Kiselev, A. V., Kiselev, S. A., and Kuznetsov, B. V., *J. Colloid Interface Sci.* **48,** 58 (1974).
13. Gay, I. D., and Liang, S., *J. Catal.* **44,** 306 (1976).
14. Klyachko, A. L., *Kinet. Katal.* **19,** 1218 (1978).
15. Lercher, J. A., Colombier, Ch., Vinek, H., and Noller, H., *Stud. Surf. Sci. Catal.* **20,** 25, 1985.
16. Spitz, R. N., Barton, J. E., Barteau, M. A., Staley, R. H., and Sleight, A. W., *J. Phys. Chem.* **90,** 4067 (1986).
17. Rossi, P. F., Busca, G., Lorenzelli, V., Lion, M., and Lavalley, J. C., *J. Catal.* **109,** 378 (1988).
18. Tanabe, K., *Stud. Surf. Sci. Catal.* **20,** 1 (1985).
19. Malinowski, S., *Stud. Surf. Sci. Catal.* **20,** 57 (1985).
20. Luy, J. C., and Parera, J. M., *Appl. Catal.* **26,** 295 (1986).
21. Knözinger, H., *Adv. Catal.* **25,** 184 (1976).
22. Cremer, E., *Adv. Catal. Rel. Sub.* **7,** 75 (1955).
23. Galwey, A. K., *Adv. Catal.* **26,** 247 (1977).
24. Taniguchi, H., Masuda, T., Tsutsumi, K., and Takahashi, H., *Bull. Chem. Soc. Japan* **52,** 2195 (1979).
25. Taniguchi, H., Masuda, T., Tsutsumi, K., and Takahashi, H., *Bull. Chem. Soc. Japan* **53,** 362 (1980).
26. Kapustin, G. I., Kustov, L. M., Glonti, G. O., Brueva, T. R., Borovkov, V. Yu, Klyachko, A. L., Rubinshtein, A. M., and Kazanskii, V. B., *Kinet. Katal.* **25,** 1129 (1984).
27. Klyachko, A. L., Bankós, I., Brueva, T. R., and Kapustin, G. I., *React. Kinet. Catal. Lett.* **29**(2) 451 (1985).
28. Benesi, H. A., and Winquist, B. H. C., *Adv. Catal.* **27,** 98 (1978).
29. Klyachko, A. L., Kapustin, G. I., Brueva, T. R., and Rubinstein, A. M., *Zeolites* **7,** 119 (1987).
30. Greppi, L., M. S. thesis, University of Wisconsin at Madison, 1987.
31. Connell, G., Unpublished results, University of Wisconsin, 1985.
32. Masuda, T., Taniguchi, H., Tsutsumi, K., and Takahashi, H., *J. Japan Petrol. Inst.* **22,** 67 (1979).
33. Auroux, A., Sayed, M. B., and Védrine, J. C., *Thermochim. Acta* **93,** 557 (1985).
34. Kapustin, G. I., Brueva, T. R., Klyachko, A. L., and Rubinshtein, A. M., *Kinet. Katal.* **22,** 1561 (1981).
35. Fubini, B., Della Gatta, G., and Venturello, G., *J. Colloid Interface Sci.* **64,** 470 (1978).
36. Stradella, L., and Venturello, G., *in* "Proceedings of the Seventh International Conference on Thermal Analysis" (B. Miller, Ed.), Vol. 2, p. 1244. Wiley, Chichester, UK, 1982.
37. Busca, G., Rossi, P. F., Lorenzelli, V., Benaissa, M., Travert, J., and Lavelley, J-C., *J. Phys. Chem.* **89,** 5433 (1985).
38. Stradella, L., *in* "Catalysis by Acids and Bases," Vol. 191. Elsevier, Amsterdam, 1985.
39. Sanderson, R. T., "Polar Covalence," Academic Press, New York, 1983.
40. Sanderson, R. T., *J. Amer. Chem. Soc.* **105,** 2259 (1983).